

L. Blumberg, J. Bittner, J. Galayda, R. Heese, S. Krinsky, J. Schuchman, and A. van Steenbergen†

**Abstract**

A 700 MeV electron storage ring designed for synchrotron radiation applications is described. Lattice and stability calculations are presented and the vacuum, correction and injection systems are discussed.

**Introduction**

The VUV electron storage ring is basically that proposed by Green and Chasman,<sup>1</sup> a 4 superperiod machine of  $C = 51.024\text{m}$  circumference, nominal energy  $E=700\text{MeV}$ , and design current  $I = 1\text{A}$ . Each quadrant, illustrated in Fig. 1, contains two  $45^\circ$  curved, C-type parallel edge bending magnets with horizontally focusing quadrupoles between the dipoles to achieve an achromatic  $90^\circ$  quadrant bend. The quadrants are connected by long straight sections of  $3.256\text{m}$  effective length with quadrupole doublets at either end. Two of the long straights are reserved for injection and RF components and two will be utilized for multipole beam undulators. Sextupole magnets are included to correct the chromaticity  $\xi = \Delta v / (\Delta p/p_0)$  to positive values to suppress the head-tail instability.<sup>2</sup> Details of the magnet systems<sup>3</sup> and injection synchrotron<sup>4</sup> are discussed elsewhere. Machine parameters are summarized in Table 1.

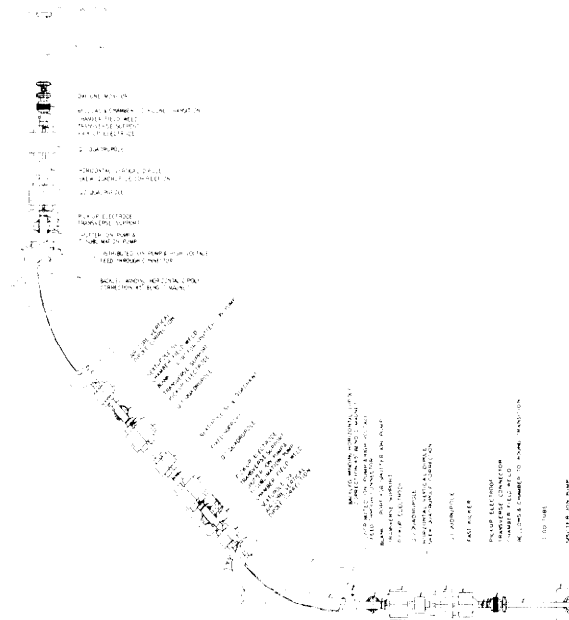


Fig. 1. Quadrant of 4-Superperiod NSLS VUV Ring.

Two photon beams are provided from each bending magnet - a  $75\text{ mrad}$  beam centered at  $17.5^\circ$  upstream and a  $100\text{ mrad}$  beam at  $0.5^\circ$  upstream of the magnet center which will yield<sup>5</sup> approximately  $1.1 \times 10^{14}$  photons/sec/mrad/1%  $\Delta\lambda/\lambda$  at the critical wavelength  $\lambda_c = 4\pi\sigma/3\gamma^3 = 31.6\text{\AA}$  and usable ( $10^{12}$ ) intensity down to  $\sim 5\text{\AA}$ . Use of undulators will provide enhanced intensity - an NSLS design<sup>6</sup> of 50 poles with  $5\text{ cm}$  wavelength gives a calculated integrated yield of  $\sim 4 \times 10^{15}$  photons/sec/mrad/1%  $\Delta\lambda/\lambda$  at  $\lambda = 200\text{\AA}$ . We have provided a  $0^\circ$  beam port from the long straight for these devices.

**I. Lattice Calculations**

The SYNCH program<sup>6</sup> has been used to calculate betatron functions and magnet strengths for machines of

Table 1. Parameters of the NSLS VUV Ring.

Energy	700 MeV	Current	1A( $1.06 \times 10^{12} e$ )
Circumference	51.024 m	Critical $\lambda$	31.6 $\text{\AA}$
Superperiods	4	Critical E	390 eV
Long straight	3.256 m	Lattice type	Sep. function
Harmonic No.	9	Charge time	90 s
No. dipoles	8	No. quads	24
Dipole field	12.226 kG	Quad grad.	Q1=47.43 kG/m
Dipole length	1.41 m (st)		Q2=33.40 kG/m
Dipole gap	55 mm		Q3=43.81 kG/m
Pole width	155 mm	Quad length	25 cm (steel)
Dipole bend	$45^\circ$	Quad apert.	10 cm
Rad curv. $\rho$	1.9098 m	Horiz. tune	$\nu_x=3.32$
Mom. compact.	.02345	Vert. tune	$\nu_y=1.32$
No. Sextupole	12	$\beta_x(\text{long str})$	11.64 m
Sext. length	17 cm	$\beta_y(\text{long str})$	5.54 m
Sext. apert.	10 cm	$\alpha_x(\text{long str})$	0
Sext. strength	$S_D = -4.81/\text{m}^2$ $S_F = +6.46/\text{m}^2$	$\alpha_y(\text{long str})$	0
RF frequency	52.880 MHz	Max. $\eta_x$	1.51 m
No. cavities	1	$\beta_x(\text{mag. cent})$	1.2 m
En. loss/turn/e	11.12 keV	$\beta_y(\text{mag. cent})$	12.4 m
Rad. power (1A)	11.3 kW*	Horiz. emitt.	$8.74 \times 10^{-6}$ mrad
Power avail.	50 kW	Vert. emitt.**	$8.8 \times 10^{-10}$ mrad
Cavity diss.	$\sim 10$ kW	Natural	$\xi_x^0 = -4.07$
Peak Voltage $\hat{V}$	100 kV	Chromaticity	$\xi_x^0 = -5.46$
Shunt imped.	$\sim 1\text{ M}\Omega$	Corrected $\xi$	$\xi_x = +3.0$
Cavity Q	$\sim 10000$		$\xi_y = +3.0$
Synch. angle	$83.6^\circ$	Rotation T	170.2 ns
Synch. freq.	12.83 kHz	Damping time	$\tau_x = 20.3$ ms
Synch. $\nu_s$	.0022		$\tau_y = 21.4$ ms
Bunch length	3.836 cm		$\tau_E = 11.0$ ms
En. sprd. $\Delta E/E$	.00044	Quantum life	$\gg 100$ h
		Touschek life	$\approx 1.5$ h***

\* Assumes 2 wigglers, En. loss=0.1 keV/wiggler/turn/e.

\*\* 10% Coupling assumed

\*\*\* For  $\hat{V}=100\text{ kV}$ . With 2x bunch length.,  $\tau_{\text{Tou}} \approx 3\text{ h}$ .

both 51 and 57 m circumference and 2 or 4 superperiods. We chose a 51 m, 4 superperiod lattice based on available space and dynamic stability. The search for solutions covered the range  $\nu_x < 5$  and  $\nu_y < 4$ . The domains  $3 < \nu_x < 4$ ,  $1 < \nu_y < 2$  and  $4 < \nu_x < 5$ ,  $2 < \nu_y < 3$  were of particular interest, and relevant results are summarized in Table 2. Criteria for selection of operating points included small emittance  $\epsilon_x$ , small  $\beta_{x,y}(\text{BEND})$  for the bending magnet sources, small uncorrected chromaticities  $\xi_{x,y}^0$ , small  $\beta_{x,y}(\text{max})$ , tunes far from integer and half integer resonances and third integral non-linear resonances  $\nu_x = n/3$  ( $n=4, 8, 12, \dots$ ) excited by the chromaticity-correcting sextupoles, and large  $\beta_{x,y}^*$  in long straights as required for coherent undulators.<sup>7</sup> Solutions near  $\nu_x, \nu_y = 3.32, 1.32$  appear optimum in these respects. The  $\beta$  and momentum dispersion functions  $\eta_x$  for this solution are shown in Fig. 2. Also of interest is the variation of tune with momentum after sextupole corrections are applied to yield positive chromaticity at  $p = p_0$ . Sextupole strengths  $S = B''L/B_0\rho$  are obtained from

$$\xi_x(y) = \xi_x^0(y) = \mp N_S \left[ N_D S_D \beta_{x,D}(y) \eta_D + N_F S_F \beta_{x,F}(y) \eta_F \right] / 4\pi \quad (1)$$

where  $N_D$  and  $N_F$  are the number of defocusing and focusing sextupoles/superperiod,  $S_D$  and  $S_F$  are their strengths,  $N_S$  is the number of superperiods, and  $\beta_{x,D}$ ,  $\beta_{y,D}$ ,  $\eta_D$  and  $\eta_F$  are the  $\beta$  and  $\eta$  functions at the indicated sextupoles. In Fig. 2 we show that  $\nu$  is a monotonic function of  $p$  and  $d\nu/dp$  remains positive in the interval  $-.01 \leq \Delta p/p_0 \leq .01$ . We thus expect stability against head-tail oscillations at injection where momentum errors of  $\pm .2\%$  are expected. Note that this solution gives smooth behavior for emittance and  $\beta$  functions vs.  $p$  whereas other operating points studied showed

\* Research supported by the U.S. Department of Energy.

† Brookhaven National Laboratory, Upton, N.Y. 11973

blow-up in  $\epsilon$  and  $\beta$  for off-momentum orbits as illustrated in Fig. 3 for  $\epsilon$ . Similar emittance blow-up was observed in a 2-fold design at  $\nu_{x,y}=3.7, 2.7$ . We have also searched for solutions with small  $\beta^*$  in the long straights for use with short wigglers. Results from Table 2 show that an operating point near  $\nu_{x,y}=4.68, 2.68$  gives small  $\beta^*$  at the expense of larger  $\epsilon$  and  $\beta$  values at the bending magnets. Stronger quads and sextupoles are also indicated and we note from Fig. 3 that the emittance blows up for  $p < p_0$ . Tune vs momentum for this solution is presented in Fig. 4. Note that  $d\nu_x/dp$  is negative for  $\Delta p/p_0 > .0035$ .

Table 2. SYNCH results,  $\nu_{x,y}=3+4, 1+2$  and  $4+5, 2+3$

$\nu_x$	3.20	3.32	3.38	3.44	3.56	3.62	3.68	3.80
$\nu_y$	1.20	1.32	1.38	1.44	1.56	1.62	1.68	1.80
$\epsilon_x \times 10^6$ (mrad)	10.6	8.7	7.9	7.1	5.7	5.0	4.5	3.6
$\beta_x^*$ (m)	11.1	11.6	12.2	12.9	15.2	17.1	19.8	30.6
$\beta_y^*$ (m)	6.1	5.5	5.3	5.1	4.9	4.9	4.9	5.6
$\beta_x$ (BEND) (m)	2.20	1.96	1.87	1.79	1.71	1.73	1.79	2.28
$\beta_y$ (BEND) (m)	14.9	14.0	13.7	13.4	13.1	13.0	13.1	14.1
$\xi_x^0$	-3.7	-4.2	-4.5	-5.0	-6.3	-7.2	-8.6	-14
$\xi_y^0$	-2.9	-3.0	-3.0	-3.1	-3.2	-3.3	-3.4	-4.0
$G_{Q1}$ (kG/m)	45.0	47.4	48.6	49.7	51.7	52.6	53.4	54.7
$G_{Q2}$ (kG/m)	30.9	33.4	34.6	35.8	38.1	39.2	40.2	42.0
$\nu_x$	4.20	4.32	4.38	4.44	4.56	4.62	4.68	4.80
$\nu_y$	2.20	2.32	2.38	2.44	2.56	2.62	2.68	2.80
$\epsilon_x \times 10^6$ (mrad)	49.0	30.5	25.6	21.9	17.0	15.2	13.7	11.3
$\beta_x^*$ (m)	.08	.12	.13	.15	.17	.18	.18	.19
$\beta_y^*$ (m)	3.23	2.43	2.20	2.02	1.74	1.62	1.51	1.32
$\beta_x$ (BEND) (m)	8.63	5.43	4.60	3.99	3.18	2.89	2.66	2.30
$\beta_y$ (BEND) (m)	16.1	15.1	15.1	15.2	15.6	15.9	16.3	17.2
$\xi_x^0$	-22	-15	-13	-12	-11	-11	-11	-11
$\xi_y^0$	-6.7	-6.6	-6.7	-6.8	-7.3	-7.6	-7.9	-8.6
$G_{Q1}$ (kG/m)	100	101	102	102	104	104	105	107
$G_{Q2}$ (kG/m)	63.5	64.8	65.5	66.2	67.2	68.3	69.0	70.3

## II. Stability Calculations

We have used a tracking program<sup>8</sup> to follow trajectories for 10,000 and, in special cases, 100,000 turns (.84x $\tau_x$  damping time) around the ring to determine aperture limits. In Table 3 we summarize maximum initial coordinate values for stable motion of on and off-energy particles for several designs: - the 4-fold doublet ring of Table 2, a C=56.7 m circumference ring with quadrupoles triplets in the long straights, and a C=51 m 2 superperiod ring with triplets in two long straight sections and doublets in the other two. The dynamic aperture of the 4-fold doublet ring exceeds the aperture of the vacuum chamber.

Table 3. Dynamic Apertures for Several VUV Designs.

INITIAL COORDINATES			4-FOLD DOUB.	4-FOLD TRIP.	2-FOLD
X	Y	E	$\nu_x=3.32$	$\nu_x=4.63$	$\nu_x=3.70$
			$\nu_y=1.32$	$\nu_y=3.58$	$\nu_y=2.71$
			$\sigma_x=0.97$ mm	$\sigma_x=0.86$ mm	$\sigma_x=0.33$ mm
			$\sigma_y=0.47$ mm	$\sigma_y=0.17$ mm	$\sigma_y=0.09$ mm
			$\sigma_E=.00043xE$	$\sigma_E=.00043xE$	$\sigma_E=.00043E$
VARY 0	0		X=100 $\sigma_x$	X=80 $\sigma_x$	X=40 $\sigma_x$
VARY 0	6 $\sigma_E$		X=100 $\sigma_x$	X=50 $\sigma_x$	X=30 $\sigma_x$
0	VARY 0		Y=190 $\sigma_y$	Y=90 $\sigma_y$	Y=40 $\sigma_y$
0	VARY 6 $\sigma_E$		Y=170 $\sigma_y$	Y=90 $\sigma_y$	Y=35 $\sigma_y$
VARY VARY 0			X=Y=80 $\sigma_{x,y}$	X=Y=50 $\sigma_{x,y}$	X=Y=25 $\sigma_{x,y}$
VARY VARY 6 $\sigma_E$			X=Y=70 $\sigma_{x,y}$	X=Y=40 $\sigma_{x,y}$	X=Y=25 $\sigma_{x,y}$

## III. Closed Orbit Corrections

Deformed orbits for several configurations of position electrodes and correction dipoles were studied<sup>9</sup> for assumed magnet position and tilt errors selected at random from Gaussian distributions of RMS width  $\sigma_{x,y}=0.125$ mm and  $\sigma_\theta=0.2$ mrad. The maximum orbit deformation without corrections was determined from 6 runs

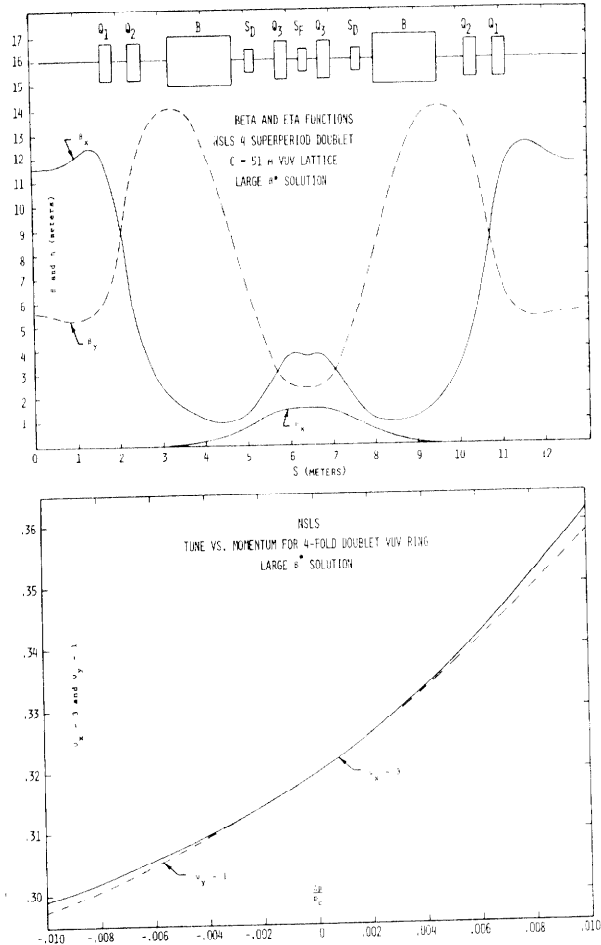


Fig. 2. (a)  $\beta$  and  $\eta_x$  functions for 1 quadrant of VUV ring at tunes  $\nu_x=3.32, \nu_y=1.32$ . (b) Tunes vs. momentum offset  $\Delta p/p_0$  with sextupoles of strength  $S_D=4.81/m^2, S_F=6.46/m^2$ .

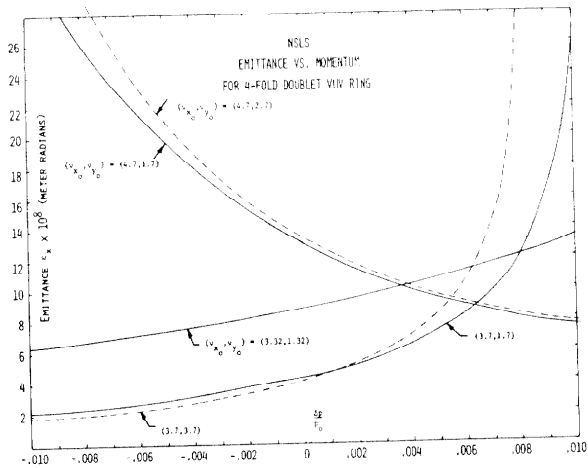


Fig. 3. Emittance vs. momentum for several operating points of the 51m, 4 superperiod VUV ring.

to be  $X_m(u)=4.79$ mm horizontal and  $Y_m(u)=3.72$ mm vertical. The correction program varies the strength of  $N_{corr}$  dipoles/superperiod by a least squares procedure to minimize the orbit error at  $N_{PUE}$  position detectors/superperiod. The maximum residual displacements  $X_m(c)$  and  $Y_m(c)$  are given in Table 4 together with the maximum required strength  $(B \times L)_c$  of correcting dipole. It is seen that the residual errors are insensitive to the number of correctors and detectors; we feel that 4 correctors and 4 detectors per superperiod are adequate

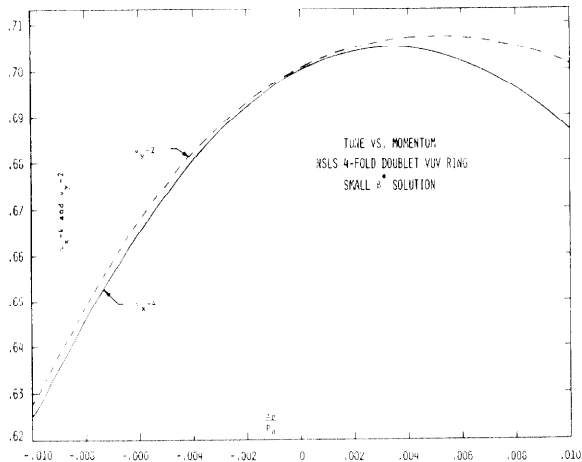


Fig. 4. Tunes vs.  $\Delta p/p_0$  for  $\nu_{x,y}=4.68, 2.68$  solution with sextupole strengths  $S_D=8.26/m^2$ ,  $S_F=8.69/m^2$ .

for this machine but will have  $N_{PUE}=6$  available for contingency. The locations of correction magnets and position detectors are indicated in Fig. 1. Backleg windings on the main dipoles will comprise half of the horizontal correctors.

Table 4. Summary of Orbit Correction Calculations

ORBIT	$N_{CORR}$	$N_{PUE}$	$X_{m(c)}/Y_{m(c)}$ (mm)	(BxL) m(c) (G-cm)
VERT.	7	7	.12	533
	6	6	.14	587
	4	6	.14	656
	4	5	.16	644
	4	4	.16	645
HORIZ.	5	7	.05	500
	5	6	.19	546
	4	6	.18	626
	4	5	.13	599
	4	4	.18	600

#### IV. Vacuum System

The vacuum enclosure is an aluminum alloy (6063-T5) extrusion which incorporates an  $80 \times 42 \text{ mm}^2$  beam chamber, an adjoining pump chamber, and integral water cooling channels as shown in Fig. 5. An extrusion of this design minimizes changes in chamber cross-section which excite higher order RF modes. The chamber sections will be field-welded to form  $90^\circ$  arcs which connect to the four straight sections with stainless steel conflat flanges. Roll-bonded aluminum-to-stainless steel transitions are used to join the aluminum chamber to the flanges. Initially, no in-line valves will be installed. The distributed pumps incorporated in the chamber within all bending magnets have an effective total pumping speed of  $2880 \text{ l/s}$ . Eight conventional sputter ion pumps are located downstream of each bending magnet, contributing an additional  $880 \text{ l/s}$ . Provisions for titanium sublimation pumps are made at these locations. Turbomolecular pumps will be used to rough the system and all control and monitoring will be via computer.

Gas desorption due to synchrotron radiation is the most significant problem in this system. For the aluminum chamber baked at  $150^\circ\text{C}$  for 24 h the gas desorption at 700 MeV and 1A is  $0.75 \text{ Tl/s}$ . Self-cleaning will reduce this value but argon glow-discharge conditioning will be used to reduce the desorption rate to  $6 \times 10^{-8} \text{ Tl/s}$  in a short time to insure an operating pressure of  $1-2 \times 10^{-9} \text{ T}$ .

#### V. Injection

The beam transfer line from the booster is displaced downward to clear the light beam lines radiating from the ring. It rises sharply to the ring level,

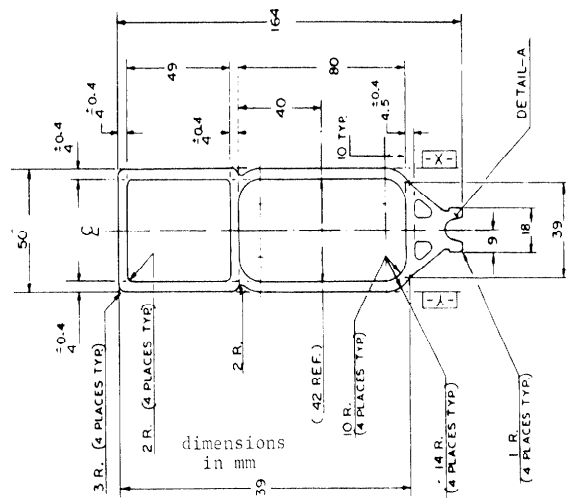


Fig. 5. Cross-section of VUV Vacuum Chamber.

where injections is accomplished by a Lambertson septum magnet. The horizontal separation between the single injected bunch and the displaced stored beam at this point will be about 10mm. The closed orbit is then retracted 28mm to its undisturbed position at a rate such that the injected bunch clears the septum when it returns due to its betatron oscillations. Injection beam dynamics were studied using the particle tracing program DIMAT.<sup>10</sup> The orbit bump will be produced by three 20-cm length full aperture ferrite kicker magnets to accommodate various tunes contemplated. Final positions are still under study.

#### VI. Acknowledgements

We thank E. D. Courant for generous support in all aspects of the lattice calculations. The expertise of H. C. H. Hsieh in design of all magnets was indispensable. We are grateful for the contributions of H. Wiedemann in beam stability and lifetime calculations and S. Ohnuma and R. Gluckstern for calculation of coupling corrections. We thank B. Culwick and J. Goldstick for design of the computer control system, J. Sheehan and G. Bagley for power supply design, and K. Batchelor and T. Dickinson for RF system design. R. Hawrylak has designed all of the ring diagnostics. Finally, we thank J. Godel for construction coordination of the building and support systems.

#### References

1. Proposal for a National Synchrotron Light Source, Ed. J. Blewett, BNL 50595, Vol. I (1977), p.4-14; R. Chasman and G.K. Green, BNL-21849 (1976); R. Chasman, G.K. Green and E.M. Rowe, IEEE Trans. Nucl. Sci. **NS-22**, 1765 (1975).
2. F.J. Sacherer, CERN Internal Report CERN/PS/BR 76-21 (1976); J. Gareyte and F. Sacherer, Proc. 9th Int. Conf. on High Energy Accel., Stanford (1974).
3. J. Galayda, et. al., paper K-14, these Proceedings.
4. J. Galayda, et. al., paper G-4, these Proceedings.
5. S. Krinsky, BNL Internal Report BNL-15698 (1976)
6. A.A. Garren and J.W. Ensco, LBL Internal Report UCID-10153 (1965); A.A. Garren and A.S. Kenney, LBL Internal Report 11/68 and 2/74. E.D. Courant has made numerous additions to SYNCH for NSLS.
7. S. Krinsky, BNL Internal Report BNL-24548 and Proc. of Wiggler Conf., Frascati, June 1978.
8. H. Wiedemann, PATRICIA code, 1977.
9. G. Parzen and K. Jellett, CLSORB code, 1978.
10. R. Servranckx, Particle Accelerators **6** (1975) 83.